Proceedings of the 2016 24th International Conference on Nuclear Engineering
ICONE24
June 26-30, 2016, Charlotte, North Carolina

ICONE24-60714

EFFECT OF SOIL STRUCTURE INTERACTION ON THE SEISMIC FRAGILITY OF A NUCLEAR REACTOR BUILDING

Samer El-Bahey, Ph.D, P.E
Senior Seismic Engineer
Stevenson & Associates
Phoenix, AZ, USA

Yasser Alzeni, Ph.D
Associate Professor
Alexandria University
Alexandria, Egypt

ABSTRACT

In recent years, the nuclear industry and the Nuclear Regulatory Commission (NRC) have made a tremendous effort to assess the safety of nuclear power plants as advances in seismology have led to the perception that the potential earthquake hazard in the United States may be higher than originally assumed. The Seismic Probabilistic Risk Assessment (S-PRA) is a systematic approach used in the nuclear power plants in the U.S. to realistically quantify the seismic risk as by performing an S-PRA, the dominant contributors to seismic risk and core damage can be identified. The assessment of component fragility is a crucial task in the S-PRA and because of the conservatism in the design process imposed by stringent codes and regulations for safety related structures, structures and safety related items are capable of withstanding earthquakes larger than the Safe Shutdown Earthquake (SSE). One major aspect of conservatism in the design is neglecting the effect of Soil-Structure-Interaction (SSI), from which conservative estimates of In-Structure Response Spectra (ISRS) are calculated resulting in conservative seismic demands for plant equipment.

In this paper, a typical Reactor Building is chosen for a case study by discretizing the building into a lumped mass stick model (LMSM) taking into account model eccentricities and concrete cracking for higher demand. The model is first analyzed for a fixed base condition using the free field ground motion imposed at the foundation level from which ISRS are calculated at different elevations. Computations taking into account the SSI effects are then performed using the subtraction method accounting for inertial interactions by using frequency dependent foundation impedance functions depicting the flexibility of the foundation as well as the damping associated with foundation-soil interaction. Kinematic interactions are also taken into account in the SSI analysis by using frequency dependent transfer functions relating the free-field motion to the motion that would occur at the foundation level as the presence of foundation elements in soil causes foundation motions to deviate from free-field motions as a result of ground motion incoherence and foundation embedment.

Comparing the results of the seismic response analyses, the effects of the SSI is quantified on the overall seismic risk and the SSI margin is calculated. A family of realistic seismic fragility curves of the structure are then developed using common industry safety factors (capacity, ductility, response, and strength factors), and also variability estimates for randomness and uncertainty. Realistic fragility estimates for structures directly enhances the component fragilities from which enhanced values of Core Damage Frequency (CDF) and Large Energy Release Frequency (LERF) are quantified as a final S-PRA deliverable.

INTRODUCTION

Seismic Probabilistic Risk Assessment (S-PRA) studies have been performed in many of the US Nuclear Power Plants over the last two decades. The S-PRAs were initially performed to answer safety concerns in heavily populated areas,

then evolved to satisfy the NRC's request for information regarding severe accident vulnerabilities in Generic Letter 88-20, Supplement 4 [1]. The NRC encourages the use of PRA for making risk informed decisions and has developed a Risk-Informed Regulation Implementation Plan [2] and associated regulatory guides. Most of the initial S-PRAs performed in the US in the 1980s, contained a level of uncertainty arising from the seismic hazard and uncertainty in the fragilities of structure, systems and components (SSCs) which resulted in the spread of the level of uncertainty in the calculated Core Damage Frequency (CDF).

Following the March 2011 Great Tahoku Earthquake and its catastrophic consequences on the Fukushima Daiichi NPP, it was clear that relying on uncertainties in the design could lead to catastrophic consequences. From which, the Nuclear Regulatory Commission (NRC) established a Near Term Task Force (NTTF) to conduct a systematic review of NRC processes and regulations and to determine if the agency should make additional improvements to its regulatory system. The NTTF developed a set of recommendations intended to clarify and strengthen the regulatory framework for protection against natural phenomena. Subsequently, the NRC issued a 50.54(f) letter on March 12, 2012 requesting information to assure that these recommendations are addressed by all U.S. nuclear power plants. The 50.54(f) letter requests that licensees and holders of construction permits under 10 CFR Part 50 reevaluate the seismic hazards at their sites against present-day NRC requirements and guidance.

Advances in characterizing earthquake source, travel path, and local site effects have led to the perception that the potential free field earthquake hazard in the United States may be higher than originally assumed. The effect of SSI is yet still a major uncertainty in the seismic design of nuclear power plants.

SOIL-STRUCTURE INTERACTION OVERVIEW

The ground motion observed by any structure is different than the free field motion due to the following interactions:

• *Inertial Interaction:* Inertia developed in the structure due to its own vibrations gives rise to base shear and moment, which generates displacements and rotations of the foundation relative to the free-field due to the flexibility of the soil-foundation system. This added flexibility affects the building frequency by shifting it towards the flexible range The system overall damping is also affected by the added displacements as energy dissipation via radiation damping and hysteretic soil damping rises affecting the overall system damping.

• *Kinematic Interaction:* The presence of stiff foundation elements at or below the ground surface cause foundation motions to deviate from free-field motions as a result of ground motion incoherence, wave inclination, or foundation embedment.

Commonly used methods for capturing the SSI effects are either:

Direct Analysis: where the soil and superstructure are included in the same finite element model and analyzed as one system. This could be performed using multiple SSI software like FLUSH by representing the soil as a continuum along with foundation elements. The direct analysis method is rarely used in practice due to the computational complexity.

Substructure Approach: where the structure is initially analyzed having a fixed-base, from which the dynamic characteristics of the structure are calculated including the modal frequencies, Eigen vectors, and Eigen values. The kinematic effects are then addressed using frequency dependent transfer functions relating the free-field motion to the foundation input motion (FIM) taking into account the soil column properties. The inertial interactions are then addressed by calculating frequency dependent impedance functions to represent the stiffness and damping of the soil-foundation interface depending on the soil column properties. The superposition inherent in a substructure approach requires an assumption of linear soil and structure behavior, although in practice this requirement is often followed only in an equivalent-linear sense.

SEIMSIC FRAGILITY ANALYSIS METHODOLOGY

The seismic fragility of a structure or equipment is defined as the conditional probability of its failure at a given value of acceleration (i.e., peak ground acceleration or peak spectral acceleration at different frequencies). The objective of a fragility evaluation is to estimate the capacity of a given component relative to a ground acceleration parameter. The methodology for evaluating seismic fragilities of structures and equipment is documented in the PRA Procedures Guide [3] and is more specifically described for application to NPPs in the EPRI Methodology for Developing Seismic Fragilities [4].

Fragility curves for an element corresponding to a particular failure mode can be expressed in terms of the best estimate of the median ground acceleration capacity, A_m, and two random variables lognormally distributed with logarithmic standard deviations for randomness, β_R, and uncertainty, β_U. At any peak ground acceleration value, a, the fragility, P_f, at any non-exceedance probability level, Q, can be represented by a subjective probability density function [5] and [6].

$$p_f = \left(\frac{\ln(a / A_m) + \beta_u \Phi^{-1}(Q)}{\beta_R} \right) \qquad (1)$$

where $\Phi(.)$ is the standard Gaussian cumulative distribution function. Per the equation above, probability functions of discrete values of non-exceedance probability level (Q) such as 5%, 50%, 95% can be developed resulting in a family of fragility curves for different failure modes of structures or equipment.

Fragility can also be represented in terms of total variability, β_C, as follows:

$$P(A \le a) = \Phi\left(\frac{1}{\beta_C}\ln(\frac{a}{A_m})\right) \qquad (2)$$

where;

$$\beta_C = \sqrt{\beta_R^2 + \beta_U^2} \qquad (3)$$

Seismic capacities of SSCs, could be represented by a High Confidence, Low Probability of Failure (HCLPF). The HCLPF capacity value is defined as the ground acceleration corresponding to a 5% probability of failure ($P_f = 0.05$) on the 95% confidence of non-exceedance curve calculated per Eqn. 1, or a 1% probability of failure ($P_f = 0.01$) on the mean fragility curve calculated per Eqn. 3. The HCLPF capacities equations can then be rearranged into the following equations:

$$A_{HCLPF} = A_m e^{-1.645(\beta_R + \beta_U)} \qquad (4)$$

$$A_{HCLPF} = A_m e^{-2.326(\beta_C)} \qquad (5)$$

HYBRID METHOD

The fragility methodology of estimating the median, A_m and β_R and β_U described requires the median factors of safety for different variables affecting the response and capacity to be estimated as well as their logarithmic standard deviations. In the U.S. nuclear industry, seismic margin assessments have been done for a number of nuclear power plants. Seismic margin is defined as the HCLPF capacity of the plant safe shutdown systems relative to the design basis or safe shutdown earthquake (DBE or SSE). The HCLPF capacity of the weakest link component in the safe shutdown path is considered the plant level HCLPF capacity. The HCLPF capacities are calculated using a deterministic procedure called Conservative Deterministic Failure Margin (CDFM) method which is extensively described in Ref. [7]. In order to simplify the seismic PRA, a hybrid method is suggested in Ref.'s [4] and [8]. The main feature of this method is the development of seismic fragility using the HCLPF capacity. First, the HCLPF capacity of the component is determined using the CDFM method. Next, the logarithmic standard deviation, β_C, is estimated using procedures described in Ref. [4]. For structures, β_C typically ranges from 0.3 to 0.5 with a recommended value of 0.4 for a conservative estimate [4]. The median capacity is calculated using Eqn. (5) and an approximate mean fragility curve for the component is thereby obtained. Reference [4] further recommends that this approximate fragility method initially be used for each component in the systems analysis to identify the dominant contributors to the seismic risk (e.g., core damage frequency). For the few components that dominate the seismic risk, more accurate fragility parameter values should be developed and a new quantification done to obtain a more accurate mean core damage frequency and to confirm that the dominant contributors have not changed.

Computing fragility curves for different confidence levels requires values of β_R and β_U. Using the composite variability, β_C, value of 0.4, Ref. [9] proposed a methodology to estimate β_R if β_C is known:

$$\beta_R = \frac{3}{4}\beta_C \qquad (6)$$

From which, β_U can be estimated using Eqn. (3). Alternatively, it has been suggested per Ref.'s [9] and [10].that in lieu of determining β_R and β_U explicitly, it is usually conservative to assume that the sum ($\beta_R + \beta_U$) is 0.7–0.8.

FRAGILITY PARAMETERS CALCULATION

In estimating fragility parameters, it is convenient to use the factor of safety method [6]. This method works in terms of an intermediate random variable called the factor of safety. The factor of safety, F, on ground acceleration capacity above a reference level earthquake specified for design; e.g., the safe shutdown earthquake level specified for design, A_{SSE}, is defined below [11]:

$$A = FA_{SSE} \qquad (7)$$

where; A is the actual ground motion capacity. For structures, the factor of safety is typically modeled as the product of three random variables:

$$F = F_S F_\mu F_{SR} \qquad (8)$$

where; The strength factor, F_S , represents the ratio of ultimate to the stress calculated for A_{SSE}. The inelastic energy absorption factor (ductility factor), F_μ, accounts for the fact that an earthquake represents a limited energy source and many structures or equipment items are capable of absorbing substantial amounts of energy beyond yield without loss-of-function. The structure response factor, F_{SR}, is based on recognition that in the design analyses, structural response was computed using specific deterministic response parameters for the structure.

The structure response factor, F_{SR}, is modeled as a product of factors influencing the response variability as follows:

$$F_{SR} = F_{SA}F_{GMI}F_\delta F_M F_{MC}F_{EC}F_{SSI} \qquad (9)$$

where; F_{SA}, is the spectral shape factor, F_{GMI}, is the ground motion incoherence factor, F_δ, is the damping factor, F_M, is the modeling factor, F_{MC}, is the mode combination factor, F_{EC}, is the earthquake component factor, and F_{SSI}, is the soil-structure interaction factor.

Depending on the analysis procedure, many of these factors are directly accounted for in the analysis. Generic data are also available in literature for these factors if not taken into account by direct analysis [5] and [6].

REACTOR BUILDING

The chosen Reactor Building is a Seismic Category I structure consisting of two basic parts: the containment shell (CS) and internal structure (IS). The Reactor Building is designed to be structurally independent of any other building with a minimum 3 inch isolation gap. Additionally, the shell and internal structure are designed to be structurally independent of each other however supported on a common base mat.

The containment shell consists of a 140 feet (inside diameter) right cylindrical wall 4 feet in thickness closed on top by a hemispherical dome 3 feet in thickness. The wall, dome, and internal structures are supported on a circular base slab 10 feet in thickness with a central cavity and instrumentation tunnel. The containment shell is constructed of concrete and pre-stressed by post-tensioned tendons in the cylindrical wall and dome. The base slab is constructed of conventionally reinforced concrete. The interior face of the containment was lined with 1/4" thick steel plates welded to form a leak-tight barrier.

The Internal Structure includes the following major components: Primary shield wall and reactor cavity, Secondary shield walls, Refueling canal walls, Operating and intermediate floors, Equipment supports (including the reactor, steam generators, reactor coolant pumps, pressurizer, and polar crane), Service platforms, Simplified head assembly with Reactor missile shield, Polar crane support system.

Shield structures are constructed of reinforced concrete. Floors are constructed of reinforced concrete or steel grating, both on structural steel framing. Support is provided by the walls of the refueling pool, the secondary shield walls, and the reactor building shell, which allows for differential movement between the shell and internal structure. The Refueling canal walls are constructed of reinforced concrete at a minimum 4 feet in thickness and lined with 1/4" stainless steel plates welded to supporting beams.

The internal structures are isolated from the shell by means of an isolation gap to minimize interaction. Where connections are used to vertically support structural steel floor framing of the internal structure to the shell, independent horizontal movement is allowed.

SITE CONDITIONS AND SEISMISITY

The chosen site is located in an area with surface bedrock consisting of alternating layers of Pennsylvanian age shales, limestones, sandstones, and a few thin coal seams. Residual soils ranging in thickness from 0 to 16 feet have been developed on the Pennsylvanian strata. Quaternary alluvium, which reaches a thickness of approximately 25 feet, is present in the tributary valleys, and scattered Tertiary age deposits of clayey gravel cap some of the higher hills in the site area.

The chosen site is located in a seismically stable region of the central United States. The nearest shocks have had intensities no greater than Modified Mercalli Intensity (MMI) III. The major zone of seismicity in the region surrounding the site is associated with the Nemaha Uplift and adjacent Central North American Rift System (CNARS). At least four MMI VII earthquakes have been associated with the Nemaha Uplift (Manhattan, 1867; Eastern Nebraska, 1877; Manhattan, 1906; Tecumseh, 1935).

SITE-SPECIFIC GROUND MOTION

In accordance with the 50.54(f) letter and following the guidance in the SPID [12], a probabilistic seismic hazard analysis (PSHA) was completed in a separate effort using the recently developed Central and Eastern United States Seismic Source Characterization (CEUS-SSC) for Nuclear Facilities (CEUS-SSC, 2012) together with the updated EPRI Ground-Motion Model (GMM) for the CEUS [13]. For the PSHA, a lower-bound moment magnitude of 5.0 was used, as specified in the 50.54(t) letter. Information pertaining to the Hazard Consistent Strain-Compatible Properties for upper bound, *UB*, best estimate, *BE*, and lower bound, *LB*, soil cases are obtained from the PSHA and used herein.

The site-specific ground motion considered herein is based on the new 100,000 year return period earthquake UHRS developed as part of the PSHA effort. Artificial time histories corresponding to the UHRS are generated herein using the Stevenson and Associates SpectraSA software using random seeds for two horizontal and one vertical time histories at 5% damping and shown in Figure 1. Comparison between the UHRS and the response spectrum generated from the artificial time histories are presented in Figure 2. The fit and enveloping requirements of Ref. [14] Section 3.7.1 Option 1 Approach 2 are applied. This is not specifically required for an S-PRA but serves to ensure resulting time histories are suitable without any deficiencies of power across the frequency range of interest.

SOIL PROPERTIES

The site PSHA gives the best estimation (median) of the values of the relevant large strain soil properties, together with lower bound values and upper bound values at 10^{-5} UHRS. The data obtained from the PSHA and that given by the plant USAR report are used to build the soil profile at the location of the Reactor Building.

The soil profile is modeled up to a depth of 259 ft. where a hard rock layer (dense limestone) is present. A sensitivity study was carried considering depth up to 500 ft, it was found that considering layers below depth of 259 ft (dense limestone, shale and sand stone) does not have a significant effect on the response of the structure. Accordingly the depth of the soil profile for the three soil cases was taken to be 259 ft.

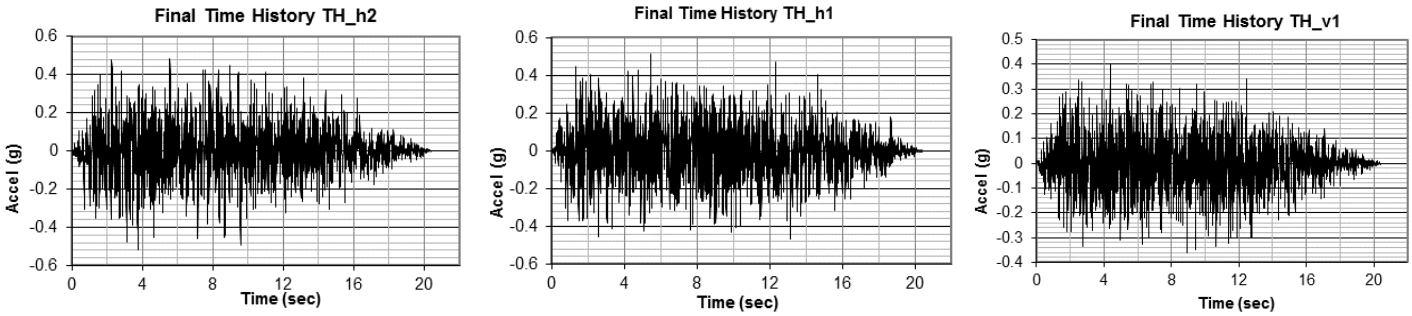

Figure 1. Artificial Time Histories Corresponding to the UHRS

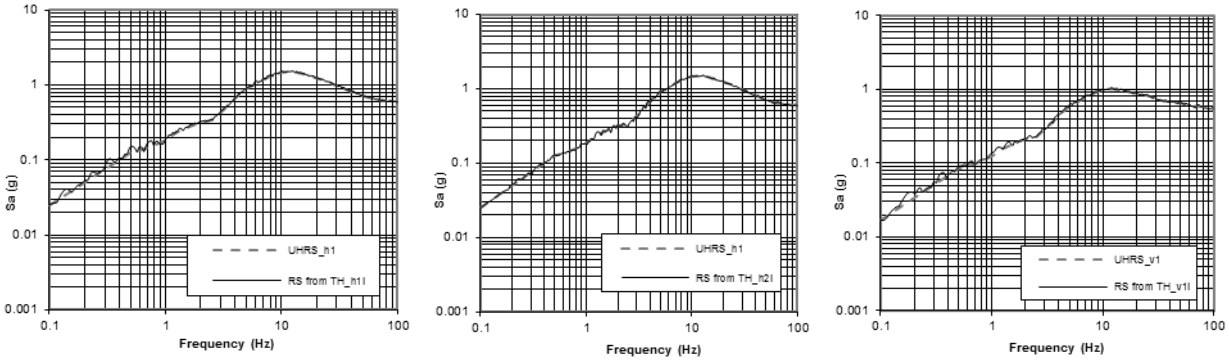

Figure 2. Comparison between the UHRS and the Response Spectrum Generated From the Artificial Time Histories

The Poisson's ratio was calculated based on the shear wave velocities values for BE, LB, and UB and the compression wave velocities from the USAR. The top of the soil profile is at the grade level, and soil properties were calculated as follows:

The low strain Poisson's ratio, ν_l, that is the same for BE, LB, and UB, is calculated based on values of the best estimate shear wave velocity at low strain, V_{sbel}, and the compression wave velocity based on low strain, V_{pbe}, as follows:

$$\nu_l = \frac{1-2\left(\frac{V_{sbel}}{V_{pbe}}\right)^2}{2-2\left(\frac{V_{sbel}}{V_{pbe}}\right)^2} \qquad (10)$$

Using low strain shear LB and UB velocity values, the strain independent upper, V_{pub}, and lower bounds, V_{plb}, for compression wave velocities were calculated as follows:

$$V_{Plb} = V_{slbl}\sqrt{\frac{2\nu_l - 2}{2\nu_l - 1}} \qquad (11)$$

$$V_{Pub} = V_{subl}\sqrt{\frac{2\nu_l - 2}{2\nu_l - 1}} \qquad (12)$$

High strain Poisson's ratios, ν_{beh}, ν_{ubh}, and ν_{lbh}, for BE, UB, and LB can then be calculated using high strain shear wave velocities respectively as follows:

$$\nu_{beh} = \frac{1-2\left(\frac{V_{sbeh}}{V_{pbe}}\right)^2}{2-2\left(\frac{V_{sbel}}{V_{pbe}}\right)^2} \qquad (13)$$

$$\nu_{uph} = \frac{1-2\left(\frac{V_{subh}}{V_{pub}}\right)^2}{2-2\left(\frac{V_{subh}}{V_{pub}}\right)^2} \qquad (14)$$

$$\nu_{lbh} = \frac{1 - 2\left(\frac{V_{slbh}}{V_{plb}}\right)^2}{2 - 2\left(\frac{V_{slbh}}{V_{plb}}\right)^2} \qquad (15)$$

High strain soil properties for the best estimate, soil case is presented in Table 1.

Table 1. Soil Properties, Best Estimate, used in SSI Analysis

Layer Thickness (ft)	Density	Shear Wave Velocity (ft/sec)	Poisson's Ratio	Damping
5	0.003299	466.8	0.47852	0.045681
5	0.003299	380.57	0.485925	0.07539
5	0.004324	1317.9	0.474654	0.046786
5	0.004324	1293.9	0.475613	0.049516
5	0.004324	1362.9	0.472798	0.049373
5	0.004324	1316	0.474731	0.051174
6	0.004324	1304.7	0.475184	0.052039
6	0.004657	5445.5	0.410868	0.034608
6	0.004657	5241.6	0.418486	0.035233
6	0.004657	4124	0.234198	0.037009
6	0.004657	4143.4	0.23034	0.03739
4	0.004657	4215	0.215593	0.037579
6	0.004657	4955.7	0.390685	0.036397
6	0.004657	5098.2	0.382813	0.036477
6	0.004657	4977.4	0.389513	0.036962
3	0.004727	4411.7	0.264807	0.038422
18	0.004727	4100.8	0.309004	0.040044
18	0.004727	3920.5	0.330983	0.041528
18	0.004727	3896.4	0.333743	0.040127
18	0.004727	3871.6	0.336542	0.040664
18	0.004727	3942.3	0.328451	0.040906
18	0.004727	4003.8	0.321127	0.041099
18	0.004727	3910.3	0.332156	0.041746
18	0.004727	3908.2	0.332397	0.0421
18	0.004727	3950.9	0.327443	0.042249
12	0.004851	4051.9	0.315206	0.042091

STRUCTURAL MODEL DESCRITIZATION

The Reactor Building is composed of four structures: the Nuclear Steam Supply System (NSSS), the Internal Structure (IS), Reactor Vessel (RV), and the Containment Shell (CS). These four structures share the same foundation; however, the CS is considered as an independent structure, whereas the NSSS and RV are coupled with the IS.

A fixed base lumped mass stick model was constructed using GT-STUDL software as shown in Figure 3 for one plane of symmetry using beams representing the containment walls above the ground surface as well as the internal walls, reactor internals, and floors. Spring elements with displacement and rotational stiffnesses were also used to model the lateral supports for the reactor vessel and the steam generator. Concrete stick elements were anticipated to be significantly cracked at the review level earthquake (RLE). Reductions in stiffness parameters for these elements were incorporated per the guidance of ASCE 4-13 Table 3-1 [15]

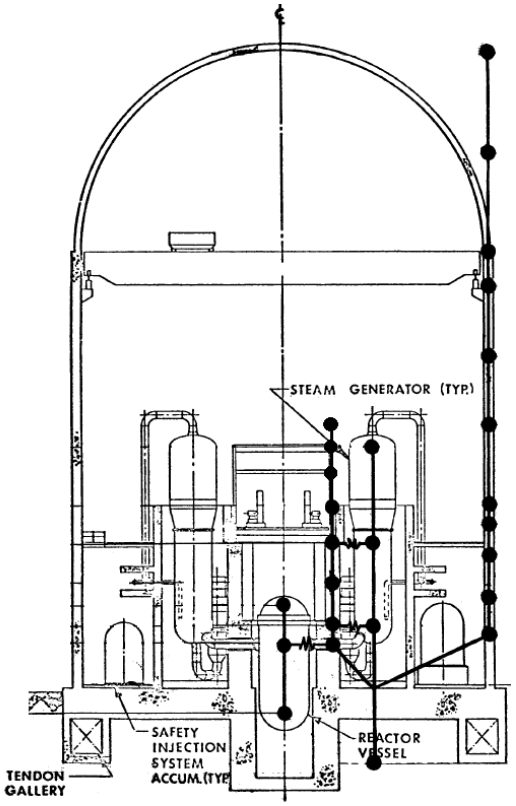

Figure 3. Reactor Building Fixed Base Lumped Mass Stick Model

CONCRETE CRACKING

Cracking assessment was performed on the CS and the IS to determine whether the major concrete elements crack under the 1E-5 UHRS loading from which adjustments to building stiffness are necessary to obtain realistic building responses. The review level cracking at each floor was determined by scaling the design basis shear stresses and comparing to the cracking threshold of $3\sqrt{f_c'}$ per ASCE 4-13 [15]. Significant cracking below El. 2051' in the East-West direction was found, from which stiffness adjustments were applied to both horizontal directions as the shell is cylindrical by using an effective shear area and an effective area moment of inertia of elements to be equal to 50% of their nominal values.

SSI ANALYSIS

The EKSSI computer programs used herein for SSI analysis were developed by Professor Eduardo Kausel of the Massachusetts Institute of Technology (MIT), and verified by Stevenson and Associates (S&A). The EKSSI software package includes multiple modules. The following two modules were used for the current analysis. The *SUPELM* program module computes the frequency-dependent dynamic impedance of the

foundation. The foundation is assumed to be rigid and cylindrical in shape, which is reasonable. *SUPELM* can also compute transfer functions allowing for the determination of time histories at the bottom of the foundation using the *SUPELM KININT* module. The *EKSSI* program module provides the frequency domain solution, including SSI effects, to a dynamically-loaded structure that is supported on compliant soil. The *EKSSI* program performs the SSI analysis by combining the building model and the foundation impedance matrix, subjecting the combined model to input acceleration time histories, and determining the response at required nodes.

Fixed-base modal properties for the Reactor Building and the Internal Structure are calculated using *GT-STRUDL* software. The UHRS time histories applicable to the free field surface are calculated using *SPECTRASA* software.

Impedance functions for the substrata are calculated using *SUPELM*. The transfer functions are used by the *KININT* module to generate time histories at the foundation bottom.

The structural model and the foundation impedance functions are combined in *EKSSI* to form the soil-structure interaction model. The models are then analyzed in *EKSSI* using the input time histories. Resultant response time histories are calculated separately in the X, Y, and Z directions at all levels of interest. Structural inherent damping was considered at 5% accounting for cracked pre-stressed containment wall.

SEISMIC RESPONSE ANALYSIS

Two analyses are conducted on the finite elements model, namely SSI and Fixed-base analyses. The SSI analysis examines the soil-structure system using the substructure method and computes the floor response spectra associated with the SSI effects at various elevations of the structure. The fixed-base condition analyzes the same model but neglects the SSI effects. The in-structure response spectra outputs of these two analyses are compared and used to calculate the family of fragility curves for both cases from which the effect of the SSI could be quantified.

Structural inherent damping was considered at 5% taking into account the non-linear effects for cracked pre-stressed containment wall.

The vibration properties of the model are summarized in Table 2 for the two horizontal and the vertical directions. The fundamental frequency of the CS was observed at the low frequency range at 4.25Hz, however the fundamental frequency of the IS was observed at the high frequency range at 15.83 Hz.

Table 2. Vibration Properties of the Model

Mode	Frequency (Hz)	Mass Contribution (%)
Horizontal X Direction		
1st	4.25	27.3
7th	11.8	7.2
12th	15.83	11
22nd	31.93	6.6
24th	36.11	9
26th	38.89	14
34th	46.33	6.8
Horizontal Y Direction		
2nd	4.25	27.3
8th	11.8	7.14
14th	18.65	15.7
23rd	32.44	5.5
25th	36.16	8.3
27th	39.32	17.8
Vertical Direction		
11th	14.96	33.6
28th	40.15	24.3
31st	42.80	4.8
43rd	62.92	12.12
54th	73.19	17.7

Figure 4 shows a comparison between the foundation base ISRS resulting from the SSI and the FB analyses and the horizontal UHRS input. It can be seen that the UHRS input exactly matches the FB analysis ISRS as expected. However, a significant reduction is observed in the high frequency region due to the SSI effect. No significant effect was observed at the low frequency region below 3 Hz. This is due to that the seismic input has a high frequency content above 3Hz as shown in the power amplitude function in Figure 5. A ZPA of 0.363g is observed for the envelope SSI ISRS compared to 0.6g for the FB ISRS.

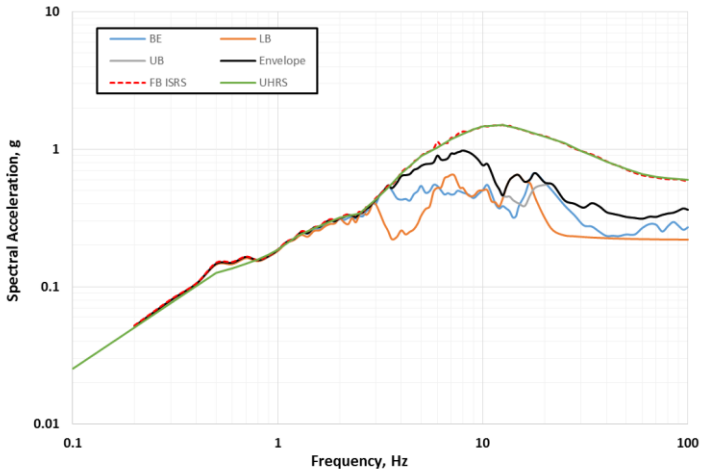

Figure 4. Comparison between the Foundation Base SSI ISRS , FB , and The Horizontal UHRS Input

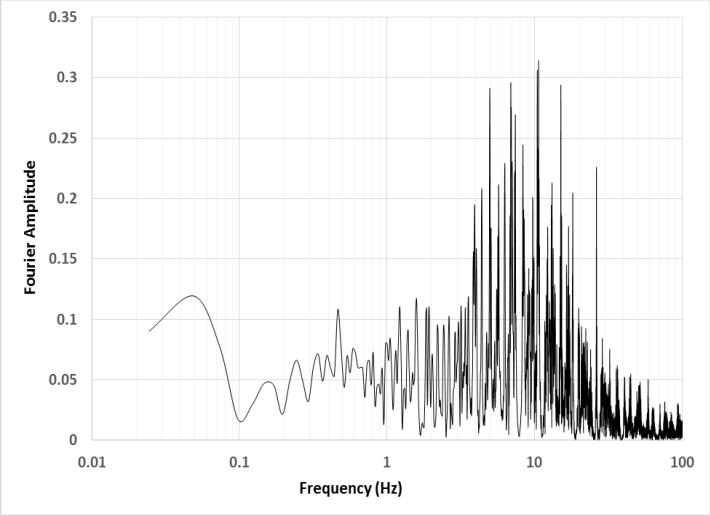

Figure 5. Fourier Amplitude of the Ground Motion

Significant ZPA reductions are expected for floors with higher fundamental frequencies mainly in the IS, however less significant benefit from the SSI is expected in floors with low fundamental frequencies as in the CS. Figure 6 shows the X direction ISRS comparison for the top of CS floor at elevation 2206'-6", and Figure 7 shows the ISRS comparison for the top of IS floor at elevation 2083'-6".

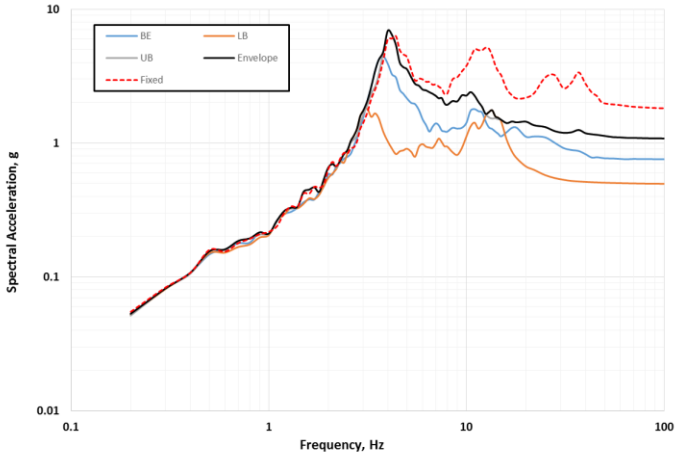

Figure 6. Horizontal Direction Comparison between SSI and FB at top of CS at Elev. 2206'-6"

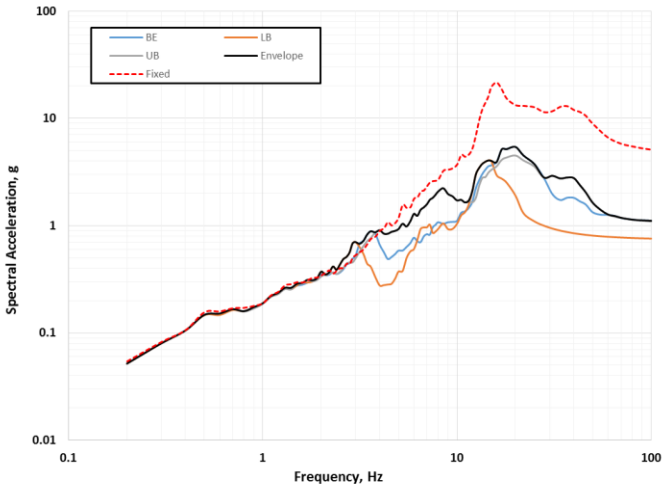

Figure 7. Horizontal Direction Comparison between SSI and FB at top of IS at Elev. 2083'-6"

Figure 8 and Figure 9 shows plots depicting the model nodes and the associated ZPA for both the CS and the IS respectively, a representation of the F_{SSI} is also represented in the plots as:

$$F_{SSI} = \frac{ZPA_{FB}}{ZPA_{SSI}} \qquad (16)$$

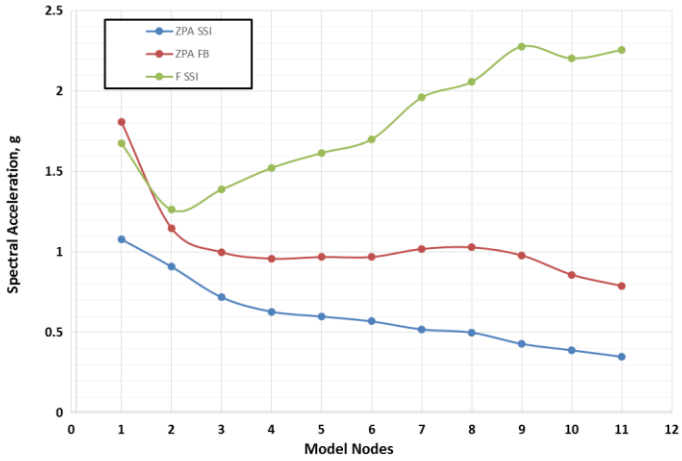

Figure 8. Containment Shell Nodal ZPA's comparison

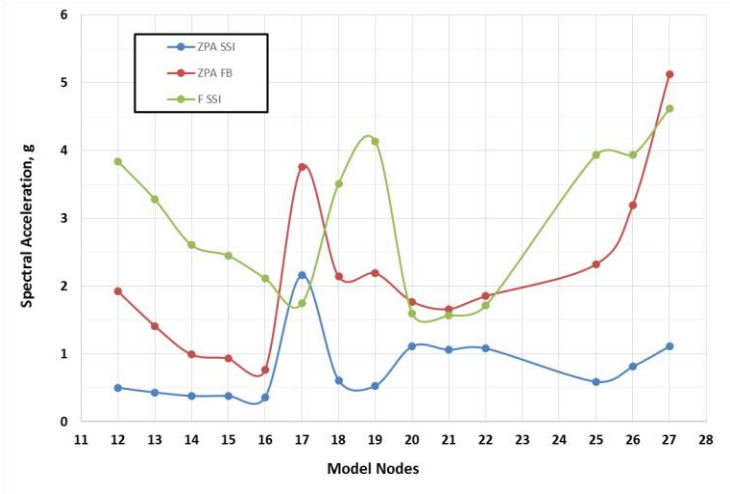

Figure 9. Internal Structure Nodal ZPA's comparison

It can be seen that the upper portions of the CS exhibits the least benefit from the SSI with a minimum F_{SSI} factor of 1.26 observed at model point 2, this is due to the low fundamental frequency compared to the high frequency content of the seismic input. The maximum F_{SSI} factor observed was at the top of the IS and equal to 4.62, the steam generator also exhibits major SSI benefit as its fundamental frequency is also in the rigid range.

FRAGILITY ANALYSIS

Evaluation of the Reactor Building design basis calculations revealed that the foundation bearing pressure is the critical failure mode with the least seismic design margin. The CDFM method is adopted here to calculate the HCLPF capacity associated with generic variability data to generate the family of fragility curves for the Reactor Building. Per CDFM, an 84% exceedance level is required for the demand. Two HCLPF values were calculated for the fixed base and the SSI conditions, from which the envelope of the response for all soil profiles is used to represent the required demand. The shear force and the associated overturning moment were calculated for each nodal mass for both cases using the ZPA of the generated ISRS. The base shear and the base moment contribution were then calculated by using the square root of the sum of the squares method for the containment shell, internal structure, and foundation shear and moment demand.

Two cases were evaluated for each of the fixed base and the SSI models for seismic upwards and seismic downwards. The upward seismic case was the controlling case for the HCLPF capacity. The strength and structure response factors are already integrated in the model, the ductility factor, F_{μ}, is taken equal to 1.0 as the failure mode is bearing pressure and is non ductile. The Analysis revealed HCLPF values of 0.74g for the SSI case and 0.47g for the fixed base case.

An average quantification of the F_{SSI} factor can be calculated assuming all other factors are not changed between the two cases as:

$$F_{SSI} = \left(\frac{A_{HCLPF\_FB}}{A_{HCLPF\_SSI}} \right) \qquad (17)$$

An average value of F_{SSI}=1.6 was calculated, this is in lieu with the range of median values observed for the SSI effect in literature [5] and [6].

The overall fragility curves are computed and plotted for five confidence levels and a mean fragility curve in. Figure 10 and Figure 11 for SSI and Fixed base analysis respectively. Median acceleration values and HCLPF values are presented in Table 3 for the fixed base and the SSI fragility analyses.

Table 3. . Median Acceleration Values and HCLPF

	β_C=0.4 β_R=0.3 β_U=0.26	
Acceleration	Fixed Base	SSI
A_{HCLPF}=	0.47g	0.74g
A_m=	1.18g	1.87g
A_{95}=	0.77g	1.22g
A_{84}=	0.91g	1.44g
A_{16}=	1.53g	2.43g
A_{05}=	1.81g	2.87g

In order to illustrate the effects of SSI on the total fragility curves, fixed-base fragility curves are compared to the SSI fragility curves. Figure 12 compares the mean and 50% confidence level fragility curves of SSI with those of the fixed-base condition.

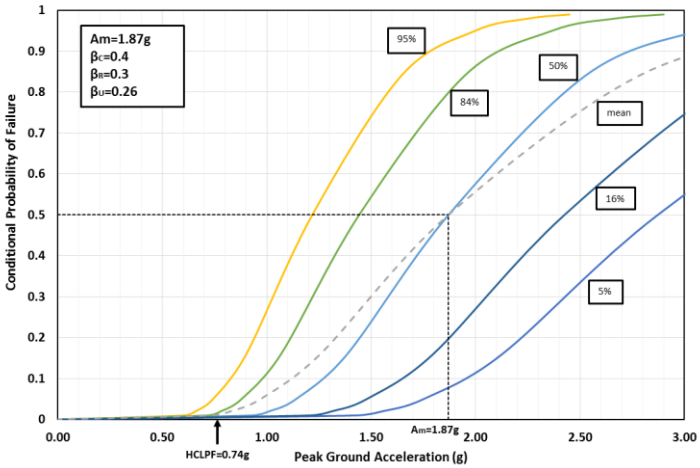

Figure 10. Fragility Curves for Reactor Building with SSI

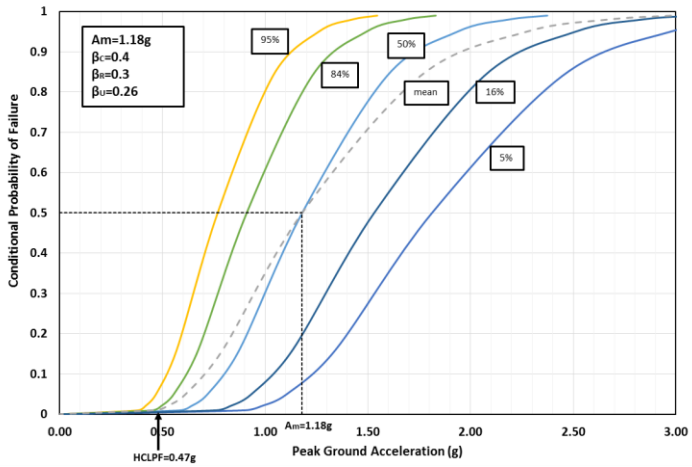

Figure 11. Fragility Curves for Reactor Building with Fixed Base

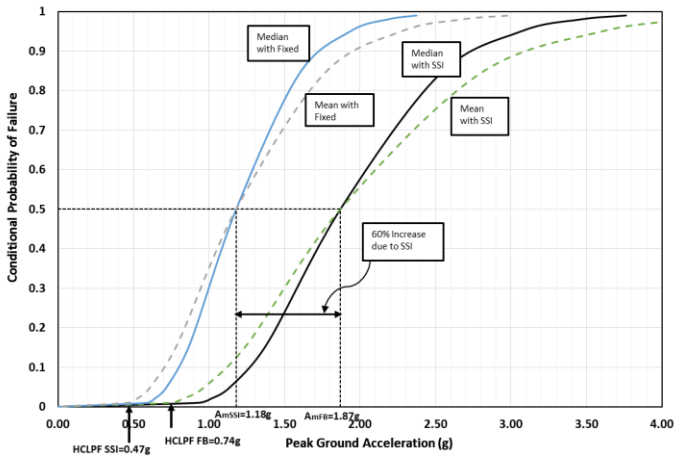

Figure 12. Comparison between Median and Mean fragilities for the Reactor Building with and without SSI

As seen from the figure, the SSI fragility curves are located to the right of the fixed-base fragility curves and cover wider range of acceleration (e.g. mean curve covers the acceleration range from 0 to 4 g to reach the 100% probability of failure compared to the 2.5 g acceleration range in the fixed-base condition). The median acceleration due to SSI is equal to 1.87g compared to 1.18g from the fixed base, this is a 1.6 factor. Giving credit to the SSI effects, the probability of damage occurrence is decreased and larger ground motions can be resisted by the structure.

CONCLUSION

The S-PRA is a systematic approach used in the nuclear power plants in the U.S. to realistically quantify the seismic risk. The assessment of component fragility is a crucial task in the S-PRA and because of the conservatism in the design process structures and safety related items are capable of withstanding earthquakes larger than the SSE. SSI is considered a major aspect of conservatism. In this paper, a typical Reactor Building is analyzed for a fixed base condition and also taking into account the SSI effects. Comparing the results of the seismic response analyses, the effects of the SSI is quantified on the overall seismic risk and the SSI margin is calculated. A realistic seismic fragility of the structure is then computed and related fragility curves are developed.

REFERENCES

1. USNRC., *Supplement 4, Individual Plant Examination of External Events (IPEEE) for Severe Accident Vulnerabilities—10CFR 50.54 (f)(Generic Letter No. 88-20).* US NRC, Rockville, 1991.
2. USNRC, *Risk-Informed Regulation Implementation Plan*. 2000, Washington, DC: Document US NRC SECY-00-213.
3. USNRC, PRA Procedure Guide. *NUREG/CR-2300.* USNRC, 1983. **1**: p. 6-43.
4. Kennedy, R. and J. Reed, *Methodology for Developing Seismic Fragilities'*. 1994, EPRI TR-103959, Electric Power Research Institute, Palo Alto, CA.
5. Kennedy, R.P., et al., *Probabilistic seismic safety study of an existing nuclear power plant.* Nuclear Engineering and Design, 1980. **59**(2): p. 315-338.
6. Kennedy, R. and M. Ravindra, *Seismic fragilities for nuclear power plant risk studies.* Nuclear Engineering and Design, 1984. **79**(1): p. 47-68.
7. Reed, J., et al., *A methodology for assessment of nuclear power plant seismic margin*. 1991, Electric Power Research Inst., Palo Alto, CA (United States); Benjamin (JR) and Associates, Inc., Mountain View, CA (United States); Structural Mechanics Consulting, Inc., Yorba Linda, CA (United States); Pickard, Lowe and Garrick, Inc., Newport Beach, CA (United States); California Univ., Davis, CA (United States). Dept. of Civil Engineering; Southern Co. Services, Inc., Birmingham, AL (United States).
8. Kennedy, R.P. *Overview of methods for seismic PRA and margin analysis including recent innovations*. in *Proceedings of the OECD-NEA Workshop on Seismic Risk*. 1999.
9. Ellingwood, B., *Validation of seismic probabilistic risk assessments of nuclear power plants*. 1994, Nuclear Regulatory Commission, Washington, DC (United States). Div. of Engineering; Johns Hopkins Univ., Baltimore, MD (United States). Dept. of Civil Engineering.
10. Prassinos, P., M. Ravindra, and J. Savy, *Recommendations to the Nuclear Regulatory Commission on trial guidelines for seismic margin reviews of nuclear power plants.* Lawrence Livermore National Laboratory, NUREG/CR-4482, 1986.

11. Campbell, R., G. Hardy, and K. Merz, *Seismic fragility application guide.* Final report TR-1002988, EPRI, Palo Alto, 2002.
12. *Seismic Evaluation Guidance: Screening, Prioritization and Implementation Details (SPID) for the Resolution of Fukushima Near-Term Task Force Recommendation 2.1: Seismic.* EPRI 1025287, Palo Alto, CA: 2012, 2012.
13. *Ground-Motion Model (GMM) Review Project.* EPRI 3002000717, June 2013
14. Commission, N.R., *NUREG-0800,".* Standard Review Plan for the Review of Safety Analysis Reports for Nuclear Power Plants," June, 1987.
15. 4-13, A., *Seismic Analysis of Safety-Related Nuclear Structures and Commentary.* American Society of Civil Engineers (ASCE), 2013.